Performance of block-coded land mobile satellite systems

Chang-Ming Lee*,† and Yu T. Su

Department of Communications Engineering, National Chiao Tung University, 1001 Ta Hsueh Road, Hsinchu 30056, Taiwan

SUMMARY

Although various measurements have indicated that mobile satellite channels are not memoryless, most related coded system performance analysis assumes perfect interleaving is in place so that the effect of channel memory can be completely ignored. This paper presents a systematic method to accurately and efficiently predict the performance of errors-and-erasures or errors-only decoders for block-coded systems in general mobile satellite channels. Numerical results are provided to validate our analytic results. Copyright © 2008 John Wiley & Sons, Ltd.

1. INTRODUCTION

In the past two decades, there has been a series of investigations on land mobile satellite (LMS) channel measurements and modeling. Measurements ranging from very high frequency to *Ka*-band have been performed and some statistical models were proposed [1–3]. Initial efforts were focused on the measurements and the characterization of field strength statistics but subsequent studies found that signals propagating through a mobile satellite channel often suffer from correlated fading and the received waveform variation can be modeled by a proper Markov or semi-Markov process. For different environments and applications, LMS channels can be described by a simple two-state Gilbert–Elliott (GE) model [4–7] or a more complicated multiple-state model [8–11].

Lutz *et al.* [4] suggested an analog channel model and a two-state GE model to represent *L*-band LMS channels. They also discuss the block error probability density (probability

---

*Correspondence to: Chang-Ming Lee, Department of Communications Engineering, National Chiao Tung University, 1001 Ta Hsueh Road, Hsinchu 30056, Taiwan.
†E-mail: cmlee.cm89g@nctu.edu.tw

of m errors occurring in a block of n bits), error gap distribution, and block error probability. Sebastiao *et al.* [5] extended the work of [4], evaluating the performance of Tomlinson–Cercas–Hughes codes in LMS channel through computer simulations. Zhu and Roy [6] use a two-state GE model (shadowed, unshadowed) to investigate the performance of a hybrid FEC/ARQ system in LMS channels. Ernst *et al.* [7] show the potential improvement for satellite multicast by using packet level coding in two-state *Ku*-band channels.

Vucetic and Du [8] used a linear combination of lognormal, Rayleigh, and Ricean models to describe signal variations over areas with constant environmental attributes. A finite-state Markov chain is applied to represent environmental parameter variations. Lin *et al.* [9] proposed a three-state (blocked, shadowed, clear) Markov chain to predict propagation statistics of the LMS communication in *L*- and *S*-bands. Braten and Jelta [10] characterized *L*-band LMS channels by two- or three-state (open, shadowed, or blocked) semi-Markov models where the duration in each state follows an exponential distribution. Shen *et al.* [11] presented a six-state Markov model for LMS channels with two main channel states used to describe low shadowing and high shadowing situations while each state in turns contains three sub-states.

Performance of some special or general block codes in finite-state Markov channels has been analyzed [12–16] but none deals with systems operating in LMS channels. We present a detailed performance analysis that accurately predicts the performance of general bounded-distance errors-and-erasures (EE) and errors-only (EO) decoders over correlated LMS channels. The rest of this paper is organized as follows. General two-state Markov channel model and its extension to LMS channel modeling are described in the following section, so are the related parameters. Section 3 focuses on the evaluation of the codeword error probabilities (CEPs). We first review a general CEP expression given in [17], which is in turn decomposed into some conditional CEPs. As the CEP formula involves the probability of an error event in an arbitrary s-state Markov chain, we present two algorithms for evaluating this probability. Specific expressions of each conditional CEP for the LMS channel of interest are then derived. Numerical examples and related discussion are provided in Section 5. Finally, Section 6 summarizes our major results.

2. HIDDEN MARKOV CHANNELS AND MODELS

We begin with a brief review of the classical GE model and associated parameters. We then investigate the LMS channel where the simple GE model is not sufficient to describe the channel characteristic. The effect of finite interleaving size is taken into account as well.

2.1. GE channel model

The GE channel model is a two-state Markov chain consisting of a good state G and a bad state B; see Figure 1. The transition probabilities that the channel moves from state G to state B and from state B to state G are denoted by b and g, respectively. Oftentimes, one has small values for the transition probabilities b and g. The method of matching GE channel model to a flat Rayleigh fading channel is discussed in [18]. Denoting by γ the instantaneous signal-to-noise ratio (SNR) and choosing a level γ_t for the particular instantaneous SNR value or the normalized received signal strength that separates the good state from the bad state [19] and
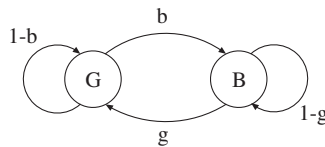
Figure 1. The Gilbert–Elliott channel model.

then matching the average bad state duration, derived from the level-crossing rate, to the average number of time units the GE channel stays in the bad state, we arrive at [18,20]

$$g = \frac{\rho f_{\mathrm{D}} T_s \sqrt{2\pi}}{\mathrm{e}^{\rho^2} - 1} \tag{1a}$$

$$b = \rho f_{\mathrm{D}} T_s \sqrt{2\pi} \tag{1b}$$

where f_{D} is the Doppler frequency, T_s is the symbol duration, and $\rho = \gamma_t/\overline{\gamma}$ is the ratio between the channel state threshold and the average SNR of the received signal. Note that the product $f_{\mathrm{D}} T_s$, which will be called *normalized fade rate* henceforth, determines the average fade rate in the sense that a smaller $f_{\mathrm{D}} T_s$ implies smaller transition probabilities and larger probabilities of staying at a given state. The choice of the threshold, as found by Wilhelmsson and Milstein [19], has, in many cases, little impact on the accuracy of the model if it is within a reasonable range.

Consider a block interleaver of m columns and n rows, where n is equal to the codeword length. The transmitted codeword symbols are written in by column and read out by row. We would like the interleaver depth m to be larger than or at least equal to the channel's coherent time. In practice, however, interleaver size is limited by both hardware and delay constraints. The combining effect of the interleaver–deinterleaver pair and the channel with memory is equivalent to that of a new GE channel whose transition probabilities are given by [(6)–(9), 19]

$$g' = P^\infty(G)(1 - (1 - b - g)^m) \tag{2a}$$

$$b' = P^\infty(B)(1 - (1 - b - g)^m) \tag{2b}$$

where $P^\infty(G)$ and $P^\infty(B)$ are steady-state probabilities of good state and bad state, respectively. Obviously, the larger the interleaver depth m, the greater the transition probabilities g' and b' become and the less likely the channel will stay at a given state. As a result, the correlations among the received samples become smaller.

2.2. An LMS channel model

The measurement of Lutz *et al.* [4] indicates that an LMS signal passes through shadowed and unshadowed sections and the characteristics of the switching process between two sections can be approximated by a Markov model. When no shadowing is present, the multipath (diffused) component is superimposed on the direct satellite signal, with the total received signal amplitude forming a Ricean process. The probability density function (pdf) of the instantaneous received power S is

$$P(S) = K\mathrm{e}^{-K(S+1)} I_0(2K\sqrt{S}) \tag{3}$$

where K is the Ricean factor and $I_0(\cdot)$ is the modified Bessel function of the first kind of order zero. When shadowing is present, S is Rayleigh distributed with a short-term mean S_0 that follows a lognormal distribution. In short, the instantaneous received power is governed by the two pdfs

$$P(S|S_0) = \frac{1}{S_0} e^{-S/S_0} \tag{4}$$

and

$$P(S_0) = \frac{10}{\sqrt{2\pi}\sigma \ln 10} \frac{1}{S_0} \exp\left[-\frac{(10 \log_{10} S_0 - \mu)^2}{2\sigma^2} \right] \tag{5}$$

where μ is the mean power level decrease (in decibels) and σ^2 is the corresponding variance of the power level due to shadowing. Measurements of the short-term average behavior over a large area suggest that S_0 can also be modeled as a Markov process. A multi-state model is thus needed to characterize the dynamic behavior of the shadowed satellite mobile channels [8]. However, it was also observed [8] that the variations of the lognormal component are much slower than the Rayleigh component. Therefore, it is reasonable to assume that when a transmitted codeword encounters a Rayleigh–lognormal fading, the received signal strength within a short period (e.g. a few codeword lengths) follows a Rayleigh distribution with a constant S_0.

Taking into account the fading characteristic in each section, which in our case might last for a few symbol or codeword lengths, we obtain the four-state model shown in Figure 2, where a superstate refers to the collection of states that characterize either unshadowed or shadowed fading and is equivalent to a section defined in [4]. For a given vehicular speed v (m/s) and sampling rate R (samples/s), the measured average distances in meters (m) that a vehicle remains in an unshadowed and a shadowed section (superstates), D_u (m) and D_s (m), and the average distances in samples are related by

$$D_u(\text{samples}) = \frac{1}{p_{us}} = \frac{R}{v} D_u \,(\text{m}) \tag{6a}$$

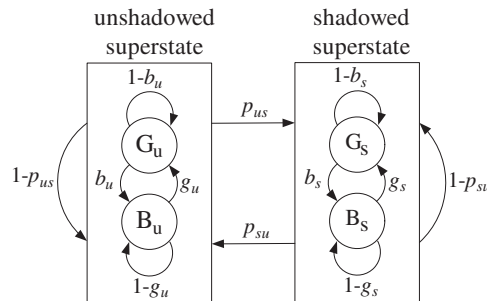$$D_s(\text{samples}) = \frac{1}{p_{su}} = \frac{R}{v} D_s \,(\text{m}) \tag{6b}$$

Figure 2. A land mobile satellite channel model.

where p_{us} and p_{su} are the transition probabilities, $P_r\{$unshadowed superstate$\rightarrow$shadowed superstate$\}$ and $P_r\{$shadowed superstate$\rightarrow$unshadowed superstate$\}$, respectively.

The transition probabilities between two superstates can be evaluated by the same method used for the GE model. Those between two shadowed (conditional Rayleigh fading) states are the same as (1a) and (1b) and are denoted by g_s and b_s, while the transition probabilities between two unshadowed states (Ricean fading) are given by

$$g_u = \frac{\sqrt{2\pi(K+1)}f_D T_s \rho e^{-K-(K+1)\rho^2} I_0(2\rho\sqrt{K(K+1)})}{1 - Q_1(\sqrt{2K}, \sqrt{2(K+1)}\rho)} \tag{7a}$$

$$b_u = \frac{\sqrt{2\pi(K+1)}f_D T_s \rho e^{-K-(K+1)\rho^2} I_0(2\rho\sqrt{K(K+1)})}{Q_1(\sqrt{2K}, \sqrt{2(K+1)}\rho)} \tag{7b}$$

where

$$Q_1(a,b) = \int_b^\infty x e^{-(x^2+a^2)/2} I_0(ax)\, dx \tag{8}$$

is the Marcum's Q function. Usually, the inter-superstate transition probabilities are smaller than the inter-state (intra-superstate) transition probabilities. But even with a very small p_{us} or p_{su} ($<10^{-4}$) and a moderate codeword length (say 200 code symbols), the probability of at least an inter-superstate transition within a codeword is much larger than the CEP. For short codes and small p_{us} or p_{su}, the CEP is to be averaged over two conditional CEPs; each one is computed under the assumption that the received samples corresponding to a codeword suffer from multiplicative fading whose statistic is governed by the states within the same superstate. For both cases, however, the error that occurs when the channel is in a shadowed state will dominate the decoder performance.

3. CEP ANALYSIS

Our analysis on the CEP $P_w(e)$ performance of a coded LMS system in a Markovian channel whose characteristic is described in the previous section follows the approach proposed in [17]. For convenience of reference, we summarize the main results of [17] in the following subsection.

3.1. A systematic approach for computing CEP

For an s-state Markov chain, we denote by $N_i, i = 1, 2, \ldots, s$, the random variables that represent the number of times state i is visited during an n-time-unit period and by $\mathscr{E}_s \stackrel{\text{def}}{=} \times (N_1 = n_1, \ldots, N_s = n_s)$ the event that during an n-time-unit period the channel is in state j for n_j (symbol) times. Then [17]

$$P_w(e) = \sum_{\mathscr{E}_s} P_w(e|n_1, \ldots, n_s) P_n(n_1, \ldots, n_s) = \sum_{\mathscr{E}_s} P_w(e|\mathscr{E}_s) P_n(\mathscr{E}_s) \tag{9}$$

where $P_w(e|\mathscr{E}_s) = P_w(e|n_1, \ldots, n_s)$ is the conditional CEP given $\mathscr{E}_s$ and $P_n(\mathscr{E}_s) = P_n(n_1, \ldots, n_s)$ is called the channel state-sequence (CSS) probability.

For a system that employs a block code of length n for transmission over a Hidden Marker Channel (HMC) characterized by an s-state Markov chain, the corresponding CEP expression

(9) is modified as

$$P_w(e) = \sum_{n_1=0}^{n} \sum_{n_2=0}^{n-n_1} \cdots \sum_{n_{s-1}=0}^{n-\sum_{j=1}^{s-2} n_j} P_n(\mathscr{E}_s) P_w(e|\mathscr{E}_s) \tag{10}$$

If the minimum distance of the code be $d_{\min} = 2t + 1$, then for EO decoding, we have the decomposition

$$P_w(e|\mathscr{E}_s) = \sum_{t=\lceil d_{\min}/2\rceil}^{n} \sum_{t_1} P_s(t_1|n_1) \sum_{t_2} P_s(t_2|n_2) \cdots \sum_{t_{s-1}} P_s(t_{s-1}|n_{s-1}) P_s(t_s|n_s) \tag{11}$$

where $t = \sum_{i=1}^{s} t_i$, $n_s = n - \sum_{j=1}^{s-1} n_j$, and $\lceil x \rceil$ represents the smallest integer greater than or equal to x, while $P_s(t_i|n_i)$ is the conditional probability that t_i errors occur during the n_i times the channel stays at state i. The upper and lower limits of various summations in (11) given above can be found in [17].

If an EE decoder is used, we have

$$P_w(e|\mathscr{E}_s) = \sum_{\ell=0}^{d_{\min}-1} \sum_{t=\lceil (d_{\min}-\ell)/2\rceil}^{n-\ell} P(\ell, t|\mathscr{E}_s) + \sum_{\ell=d_{\min}}^{n} P_E(\ell|\mathscr{E}_s) \tag{12}$$

where $P(\ell, t|\mathscr{E}_s)$ is the joint (conditional) probability that there are ℓ erasures and t errors in a codeword and $P_E(\ell|\mathscr{E}_s) = P(\ell, 0|\mathscr{E}_s)$ is the (conditional) probability that there are ℓ erasures in a codeword. Detailed expressions for these conditional probabilities can be found in [17].

The evaluation of the above conditional probabilities, $P_E(\ell|\mathscr{E}_s)$ and $P(\ell, t|\mathscr{E}_s)$, in turn, relies on the knowledge of the following component conditional probabilities [17]:

$$P_{e|i} = P_r\{\text{a symbol is erased}|\text{channel state} = i\} \tag{13a}$$

$$P_{s|i} = P_r\{\text{a symbol is incorrectly detected}|\text{channel state} = i\} \tag{13b}$$

$$P_{c,\bar{e}|i} = P_r\{\text{a symbol is correctly detected and not erased}|\text{channel state} = i\} \tag{13c}$$

$$P_{s,\bar{e}|i} = P_r\{\text{a symbol is incorrectly detected but not erased}|\text{channel state} = i\} \tag{13d}$$

It can be shown that the above conditional probabilities satisfy $P_{e|i} + P_{s,\bar{e}|i} + P_{c,\bar{e}|i} = 1$ and $P_{s|i}(1 - P_{e|i}) = P_{s,\bar{e}|i}$.

3.2. Evaluating the CSS probability

The above equation indicates that to calculate the CEP it is necessary to evaluate the CSS probability $P_n(\mathscr{E}_s)$. This issue was not addressed in [17]. We now present two simple systematic methods for computing $P_n(\mathscr{E}_s)$ for an arbitrary finite-state Markov chain.

3.2.1. The transform domain method. Define the multi-dimensional moment generating function of the random variables $N_1, N_2, \ldots, N_s$ by

$$\Psi(z_1, z_2, \ldots, z_s) = \sum_{\substack{n_1, n_2, \ldots, n_s \\ n_1+n_2+\cdots+n_s=n}} P_n(n_1, n_2, \ldots, n_s) z_1^{n_1} z_2^{n_2} \cdots z_s^{n_s} \tag{14}$$

Then it is easy to see that the corresponding joint pdf is

$$P_n(n_1, n_2, \ldots, n_s) = \frac{1}{n_1! n_2! \cdots n_s!} \frac{\partial^n}{\partial z_1^{n_1} \partial z_2^{n_2} \cdots \partial z_s^{n_s}} \Psi(z_1, z_2, \ldots, z_s) \tag{15}$$

The moment generating function $\Psi(z_1, z_2, \ldots, z_s)$ can be computed as follows. Let $\mathbf{T} = [p_{ij}]_{s \times s}$ be the transition probability matrix of the s-state Markov chain of concern and $\pi_j, j = 1, 2, \ldots, s$, be the probability of being in state j at time $t = 1$. Then it can be shown that [13]

$$\Psi(z_1, z_2, \ldots, z_s) = \Pi_Z \mathbf{T}_Z^{n-1} \underline{1} \tag{16}$$

where $\underline{1} = [1 \ 1 \cdots 1]^{\mathrm{T}}$ and $\Pi_Z = [\pi_1 z_1 \ \pi_2 z_2 \cdots \pi_k z_s]$.

3.2.2. A direct recursive method. The second method utilizes the recursive relation [13]

$$P_{ix}(d_1, \ldots, d_s) = \sum_{y=1}^{s} P_{(i-1)y}(d_1, ..., d_x - 1, ..., d_s) p_{yx} \tag{17}$$

where p_{yx} is the (one-step) transition probability from state y to state x and $P_{ix}(d_1, \ldots, d_s)$ is the joint probability that during a period of i consecutive time intervals the channel has visited state x d_x times and is in state x at the ith time interval. The initial condition is given by

$$P_{1x}(d_1, \ldots, d_s) = \begin{cases} \pi_x & \text{if } d_x = 1 \text{ and } d_y = 0 \ \forall y \in \{1, \ldots, s\} \ \{x\} \\ 0 & \text{otherwise} \end{cases}$$

Therefore,

$$P_n(n_1, \ldots, n_s) = \sum_{x=1}^{s} \sum_{y=1}^{s} P_{(n-1)y}(\ldots, n_x - 1, \ldots) p_{yx} \tag{18}$$

It can be shown that, for an s-state Markov channel with $\sum_{i=1}^{s} n_i = n$, the (multiplicative) complexities for computing $P_n(\mathscr{E}_s)$ based on the above two methods are $O((n-1)s^4 \binom{n+s-1}{s-1})$ and $O(s^{n-1} \binom{n+s-1}{s-1})$, respectively. Hence the transform domain approach is preferred if $n \gg s$.

4. CEP PERFORMANCE OF A CODED SYSTEM

In the previous section we have presented a systematic approach and general expressions for evaluating the CEP performance of an arbitrary (n, k) block code with minimum distance $d_{\min} = 2t + 1$ in an arbitrary s-state HMC. However, the CEP is a function of several component conditional probabilities, which can be derived only if the channel statistic and decoding method are given. In this section, we derive the component conditional probabilities for a system that employs a Reed–Solomon (RS) code, block interleaver, and noncoherent M-ary orthogonal modulation.

4.1. System description and basic properties

Consider the system whose (source) data stream is first encoded by an (n, k) extended RS code and interleaved by a block symbol interleaver before being mapped into M-ary orthogonal

signals, $M = n$, say, M-ary frequency shift keying, multiple frequency shift keying, or Walsh–Hadamard-coded sequences. We assume that the received signal suffers from frequency nonselective fading, i.e. the received amplitude remains constant during a symbol period. The associated symbol error probability for an optimal noncoherent detector (matched-filter bank) is then given by [21]

$$P_s(\gamma) = \sum_{i=0}^{n-2} \binom{n-1}{i+1} (-1)^i \frac{1}{i+2} e^{-\frac{i+1}{i+2}\eta\gamma} \tag{19}$$

where $\eta = k \log_2 n/n$.

An EE decoder needs an erasure-insertion method (EIM) to determine which received symbol should be erased. We use the ratio threshold test (RTT) [22] as our EIM because of its robustness against the estimation errors of channel statistic such as noise power or SNR, i.e. the optimal threshold used in an RTT remains almost constant within a large range of operating SNR. For this test, the ratio between the largest and the second largest outputs of the noncoherent matched-filter bank is compared with the threshold τ and an erasure is inserted when this ratio is greater than τ. Using such an RTT-EIM, we have [23,24]

$$P_{c,\bar{e}}(\gamma) = \sum_{i=0}^{n-1} (-1)^n \binom{n-1}{i} \frac{\exp[-(\tau i/(\tau i+1))\eta\gamma]}{\tau i+1} \tag{20a}$$

$$P_{s,\bar{e}}(\gamma) = \sum_{i=0}^{n-2} (-1)^i \binom{n-1}{i+1} \frac{\tau(i+1)}{\tau(i+1)+1} \frac{\exp[-((\tau i+1)/(\tau(i+1)+1))\eta\gamma]}{\tau i+1} \tag{20b}$$

4.2. Coded performance in HMCs

On the basis of the above three basic equations, (19)–(20b), we now derive the performance of the RS-coded system in two HMCs. Both channels have been discussed in Section 2. We begin with the simplest one in which the transmitted signal suffers from correlated Rayleigh fading distortion and additive white gaussian noise. As a two-state GE model is sufficient to describe the channel and the pdf of the instantaneous SNR is $f(\gamma) = (1/\bar{\gamma})e^{-\gamma/\bar{\gamma}}, \gamma \geqslant 0$, we use (19), (20a), or (20b) to obtain related conditional probabilities whose expressions are similar to (11a)–(12d) of [17].

Next, we consider the LMS channels over which a Walsh–Hadamard-coded orthogonal signal is transmitted. The signal suffers from Rayleigh or Ricean distortion depending on whether a line-of-sight path is present. Figure 2 shows a four-state hidden Markov model (HMM) for this class of LMS channels. The component conditional probabilities for the two shadowed (Rayleigh-faded) states have expressions similar to those of the previous case. The two unshadowed states, however, have Ricean statistics with instantaneous received SNR γ distributed according to

$$f(\gamma) = \frac{1+K}{\bar{\gamma}} e^{-K} e^{-\frac{(1+K)\gamma}{\bar{\gamma}}} I_0\left(2\sqrt{\frac{K(1+K)\gamma}{\bar{\gamma}}}\right), \quad \gamma \geqslant 0 \tag{21}$$

Assuming noncoherent detection, we then have

$$
P_{s|G_u} = \frac{1}{P_{G_u}^{\infty}} \sum_{i=0}^{n-2} (-1)^i \binom{n-1}{i+1} \frac{(1+K)\exp[((1+K)/d_s\overline{\gamma}-1)K]}{(i+2)d_s\overline{\gamma}}
$$
$$
\times Q_1\left(\sqrt{\frac{2K(1+K)}{d_s\overline{\gamma}}}, \sqrt{2d_s\gamma_t}\right)
$$
(22a)

$$
P_{s|B_u} = \frac{1}{P_{B_u}^{\infty}} \sum_{i=0}^{n-2} (-1)^i \binom{n-1}{i+1} \frac{(1+K)\exp[((1+K)/d_s\overline{\gamma}-1)K]}{(i+2)d_s\overline{\gamma}}
$$
$$
\times \left[1 - Q_1\left(\sqrt{\frac{2K(1+K)}{d_s\overline{\gamma}}}, \sqrt{2d_s\gamma_t}\right)\right]
$$
(22b)

where

$$
d_s = \frac{1}{\overline{\gamma}} + \left(\frac{i+1}{i+2}\right)\eta
$$
(23a)

$$
P_{G_u}^{\infty} = Q_1(\sqrt{2K}, \sqrt{2(1+K)}\rho)
$$
(23b)

$$
P_{B_u}^{\infty} = 1 - Q_1(\sqrt{2K}, \sqrt{2(1+K)}\rho)
$$
(23c)

For an EE decoder that uses an RTT-EIM with threshold τ, we have

$$
P_{c,\bar{e}|G_u} = \frac{1}{P_{G_u}^{\infty}} \sum_{i=0}^{n-1} (-1)^i \binom{n-1}{i} \frac{(1+K)\exp[((1+K)/d_{ce}\overline{\gamma}-1)K]}{(\tau i+1)d_{ce}\overline{\gamma}}
$$
$$
\times Q_1\left(\sqrt{\frac{2K(1+K)}{d_{ce}\overline{\gamma}}}, \sqrt{2d_{ce}\gamma_t}\right)
$$
(24a)

$$
P_{c,\bar{e}|B_u} = \frac{1}{P_{B_u}^{\infty}} \sum_{i=0}^{n-1} (-1)^i \binom{n-1}{i} \frac{(1+K)\exp[((1+K)/d_{ce}\overline{\gamma}-1)K]}{(\tau i+1)d_{ce}\overline{\gamma}}
$$
$$
\times \left[1 - Q_1\left(\sqrt{\frac{2K(1+K)}{d_{ce}\overline{\gamma}}}, \sqrt{2d_{ce}\gamma_t}\right)\right]
$$
(24b)

$$
P_{s,\bar{e}|G_u} = \frac{1}{P_{G_u}^{\infty}} \sum_{i=0}^{n-2} (-1)^i \binom{n-1}{i+1} \frac{(1+K)\tau(i+1)\exp[((1+K)/d_{se}\overline{\gamma}-1)K]}{(\tau i+1)[\tau(i+1)+1]d_{se}\overline{\gamma}}
$$
$$
\times Q_1\left(\sqrt{\frac{2K(1+K)}{d_{se}\overline{\gamma}}}, \sqrt{2d_{se}\gamma_t}\right)
$$
(24c)

$$P_{s,\bar{e}|B_u} = \frac{1}{P_{B_u}^{\infty}} \sum_{i=0}^{n-2} (-1)^i \binom{n-1}{i+1} \frac{(1+K)\tau(i+1) \exp[((1+K)/d_{se}\bar{\gamma} - 1)K]}{(\tau i + 1)[\tau(i+1)+1]d_{se}\bar{\gamma}}$$
$$\times \left[1 - Q_1\left(\sqrt{\frac{2K(1+K)}{d_{se}\bar{\gamma}}}, \sqrt{2d_{se}\gamma_t} \right) \right] \tag{24d}$$

where

$$d_{ce} = \frac{1+K}{\bar{\gamma}} + \frac{\tau i}{\tau i + 1}\eta \tag{25a}$$

$$d_{se} = \frac{1+K}{\bar{\gamma}} + \frac{\tau i + 1}{\tau(i+1)+1}\eta \tag{25b}$$

Detailed derivations of the above equations are given in the Appendix.

5. NUMERICAL EXAMPLES AND DISCUSSIONS

In the following numerical examples, the modified Jakes model of [25] is used to simulate correlated Rayleigh fading. For correlated Ricean fading, a direct path is added.

Shown in Figure 3 is the CEP performance of a (16, 8) RS-coded system as a function of the normalized fading rate $f_D T_s$ when the average $E_b/N_0 \stackrel{\text{def}}{=} \bar{\gamma}_b$ is 15 dB and the interleaver depth is $m = 27$. We use a GE channel with the state threshold $\gamma_t = 2$ dB, i.e. 13 dB below the average SNR value to predict the decoder performance in correlated Rayleigh fading. For a fixed interleaver depth, the CEP performance improves as the channel fading becomes faster since the inter-code-symbol correlation becomes smaller accordingly. At $f_D T_s = 0.01$, $m = 27$ is then sufficient to decorrelate the channel effect and provide near-perfect-interleaving performance.
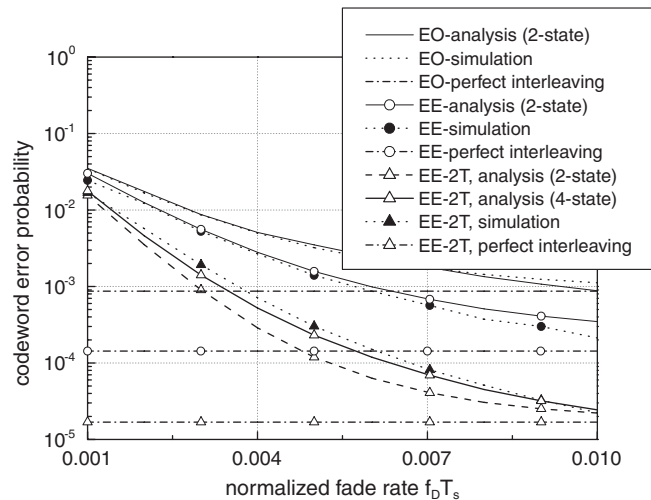

Figure 3. CEP performance of a (16, 8) RS-coded system as a function of the normalized fading rate; average $E_b/N_0 = 15$, dB, $\gamma_t = 2$ dB.

The CEPs of EE decoders using single-threshold (1T) and two-threshold (2T) RTT-EIMs [24] are also depicted in the same figure. The 2T decoder uses a state-dependent threshold to make erasure-insertion decision. The RTT has robust performance only if it operates in a stationary environment, i.e. one with time-invariant channel statistic. In a time-varying channel whose statistical properties are state-dependent, the optimal threshold should also be state-dependent. One can easily seen that (i) similar to the trend we observed in jammed channels [24], 2T EE decoding yields performance better than that of a 1T EE decoder, and (ii) the analysis based on the GE channel model gives a quite accurate performance prediction, i.e. as far as decoded CEP is concerned, GE model gives a good approximation of the channel behavior generated by the modified Jakes model. We also observe that the analytic performance prediction becomes more accurate when a four-state channel model is used. The three thresholds we used for the four-state model are 4, 0, and -4 dB, respectively. For the purpose of fair comparison, we only use two thresholds for the four-state model, i.e. the erasure-insertion threshold depends only on whether the average SNR is above 0 dB (there are two states above 0 dB and two states below).

EO and EE decoder performance of an LMS channel is shown in Figure 4. The satellite elevation angle is 24° degrees and the time-share factor of shadowing is either $A = 0.66$ (City) or 0.25 (Highway) [4]. System parameters used are carrier frequency = 1.54 GHz, data rate = 1200 symbols/s, and channel parameters associated with the former (City) case are $K = 6.0$ dB, $v = 40$ km/h, $f_D = 57.03$ Hz, $f_D T_s = 0.0475$, $D_u = 27.0$ m, and $D_s = 52.0$ meters, while those for the latter (Highway) case are $K = 11.9$ dB, $v = 90$ km/h, $f_D = 128.33$ Hz, $f_D T_s = 0.1068$, $D_u = 188$ m, and $D_s = 62.0$ m, respectively.

The normalized mean received SNR are -1.78 and -4.95 dB at Highway and City, respectively. The threshold used to separate two fading states within a superstate is 3 dB. As mentioned before, we assume that the mean received power remains constant for at least a codeword period. The performance curves thus represent a conditional performance only. The overall performance can be obtained by averaging over the lognormal distributed S_0.

Similar to the previous example, these curves indicate that our four-state HMM leads to an accurate decoder performance prediction. Since A accounts for the fraction of time the channel
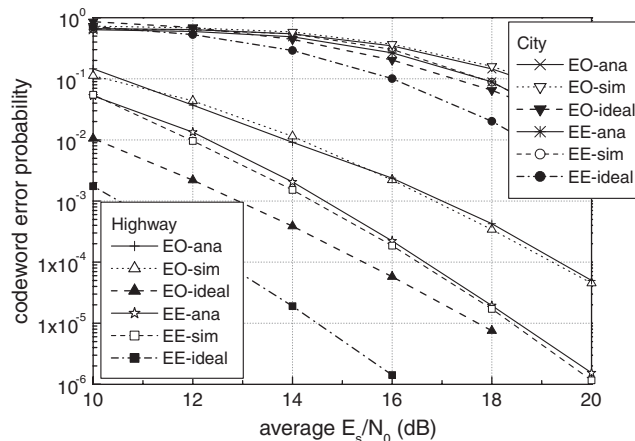

Figure 4. Simulated (sim) and analytic (ana) EO and EE decoder performance for the (16, 8) RS code over land mobile satellite channels; ideal = perfect interleaving.

stays at Rayleigh fading states, these curves imply that the EE decoding gain is more impressive in Ricean fading states.

In the remaining three figures, the decoded performance in correlated Rayleigh fading for rate 1/2 RS codes with different codeword lengths is presented. Figure 5 shows the impact of the interleaver depth m on the CEP performance of EO and EE decoders. The (16, 8) RS code is used and the threshold for the 1T RTT-EIM is 0.6. Performance for the system using a perfect (infinite interleaving size) interleaver is also given so that performance degradation due to finite interleaver size can be assessed. As expected, the larger the interleaver depth, the better the system performance. The performance of the (8, 4) and (32, 16) RS codes in correlated Rayleigh fading channels with different normalized fade rates and imperfect interleaving is depicted in Figure 7 where the interleaver size is fixed at $nm = 768$ symbols (Figures 6 and 7). For this case, the larger the codeword length n, the smaller the interleaving depth m and the higher the correlation among the received samples within a codeword length. Hence, as the performance curves in this figure indicate, for EO decoding, the longer (32, 16) code does not necessarily yield a better performance; it is even outperformed by the shorter (8, 4) code when the normalized fade rate is slow. In contrast, EE decoding is able to preserve the error-correcting capability of a more powerful code notwithstanding a small fixed finite-size interleaver. A larger normalized fade rate ($f_D T_s$) implies a faster fading and reduced correlation among the received samples. The corresponding decoder performance is thus improved.

Similar behavior can be found in Figure 8 where the performance of the (16, 8), (32, 16), and (64, 32) RS codes over LMS channels with the same channel statistics and interleaver size of Figure 4 is plotted. In a city environment, the benefit of using the longer (32, 16) codes against the shorter (16, 8) one is not clear for EO decoding. The (64, 32) codes are powerful enough to overcome the small interleaver and outperform other shorter codes for both EO and EE decoding.

When the codeword length of an RS code is greater than or equal to 64, the computational complexity of the CEP expression, (9), becomes relatively high. There are two simple ways to obtain a good approximation and reduce the complexity. We first notice that each term on the right-hand side of (9) involves a CSS probability $P_n(\mathscr{E}_s) = P_n(n_1, \ldots, n_s)$ and the corresponding
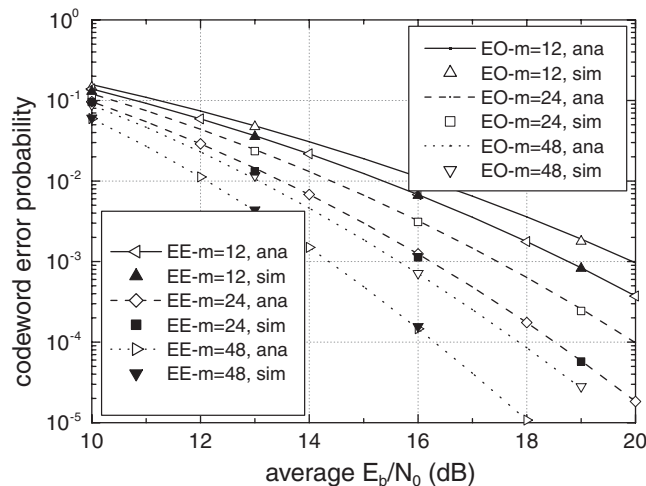

Figure 5. Codeword error probabilities as a function of the interleaver depths m.
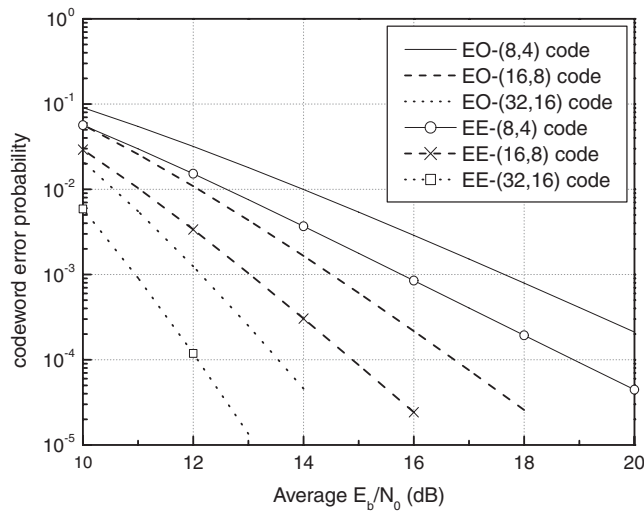
Figure 6. Codeword error probabilities as a function of the received SNR for (8, 4), (16, 8), and (32, 16) RS codes; perfect interleaving, $\tau = 0.6$ for EE decoding.
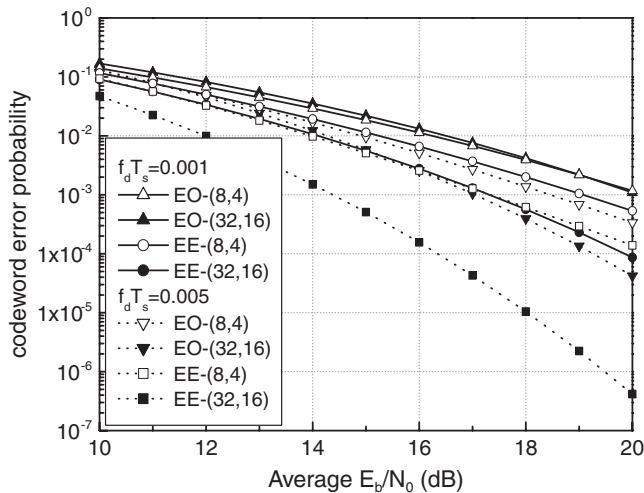

Figure 7. Codeword error probabilities as a function of the received SNR for (8, 4) and (32, 16) RS codes; $f_D T_s = 0.001, 0.005$, $\tau = 0.6$ for EE decoding.

conditional error probability $P_w(e|\mathscr{E}_s)$. Those terms with a negligible CSS probability can be neglected. Second, (11) or (12) says that the conditional error probability $P_w(e|\mathscr{E}_s)$ can be decomposed into summations of component conditional error probabilities, a proper criterion for adaptively deleting those small summands without affecting the required accuracy can be used. Our numerical experiments indicate that both methods are very efficient in reducing the computing complexity.
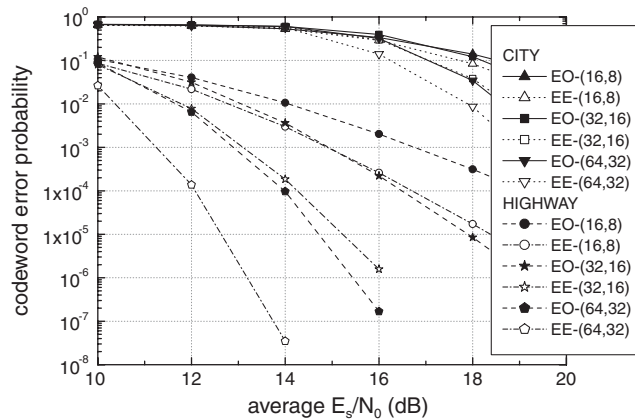
Figure 8. Codeword error probabilities as a function of the received SNR for (16, 8), (32, 16), and (64, 32) RS codes over land mobile satellite channels.

6. CONCLUSION

We have presented the performance analysis of block codes in correlated LMS channels. Using a finite-state Markov chain to model the channel in question and following the approach of [17], we develop recursive algorithms for computing the CSS probabilities, which is critical in evaluating the CEP performance of both EO and EE decoders. We consider systems that employ RS codes and M-ary orthogonal modulations. Our analysis makes it possible to study the effects of various system parameters and channel conditions on both types of decoders. These design parameters include the interleaving size, code rate, codeword length, and minimum distance and channel condition parameters such as the fade rate, average SNR, and time-share shadowing factor. Numerical results prove that our analysis does provide accurate prediction and gives performance estimation that is very close to that predicted by computer simulations using an established statistical model.

APPENDIX A

A.1. Derivations of some component conditional probabilities

This Appendix contains the derivations of the formulae of the component conditional probabilities given in Section 4.2. We choose to present only two of them as the derivations of others are similar. The first one is the conditional probability $P_{s|B}$ where B denotes that the

channel is in the shadowed superstate in which the received instantaneous SNR follows an exponential pdf:

$$f(\gamma) = \frac{1}{\overline{\gamma}} e^{-\gamma/\overline{\gamma}} \tag{A1}$$

By using (A1) and (19), we can derive the conditional probability $P_{s|B}$ as given below:

$$
\begin{aligned}
P_{s|B} &= \frac{1}{P_B^{\infty}} \int_0^{\gamma_t} f(\gamma) P_s(\gamma) \, d\gamma \\
&= \frac{1}{1 - e^{-\rho^2}} \int_0^{\gamma_t} \frac{1}{\overline{\gamma}} e^{-\gamma/\overline{\gamma}} \sum_{i=0}^{n-2} \binom{n-1}{i+1} (-1)^i \frac{1}{i+2} e^{\frac{-i+1}{i+2}\eta\gamma} \, d\gamma \\
&= \frac{1}{1 - e^{-\rho^2}} \sum_{i=0}^{n-2} (-1)^i \binom{n-1}{i+1} \frac{1}{(i+2)\overline{\gamma}} \int_0^{\gamma_t} \exp\left[-\left(\frac{1}{\overline{\gamma}} + \left(\frac{i+1}{i+2}\right)\eta\right)\gamma\right] d\gamma \\
&= \frac{1}{1 - e^{-\rho^2}} \sum_{i=0}^{n-2} (-1)^i \binom{n-1}{i+1} \frac{1 - \exp[-(1/\overline{\gamma} + ((i+1)/(i+2))\eta)\gamma_t]}{(i+2)[1 + ((i+1)/(i+2))\eta\overline{\gamma}]}
\end{aligned} \tag{A2}
$$

where

$$P_B^{\infty} = \int_0^{\gamma_t} f(\gamma) \, d\gamma = 1 - e^{-\rho^2} \tag{A3}$$

and $\rho = \gamma_t/\overline{\gamma}$.

The second example considers the case when the two unshadowed states have Ricean statistics with the received instantaneous SNR distributed according to

$$f(\gamma) = \frac{1+K}{\overline{\gamma}} e^{-K} e^{-\frac{(1+K)\gamma}{\overline{\gamma}}} I_0\left(2\sqrt{\frac{K(1+K)\gamma}{\overline{\gamma}}}\right), \quad \gamma \geq 0 \tag{A4}$$

By using (A4) and (19), we obtain the conditional probability $P_{s|G_u}$, (a), by the following steps.

$$P_{s|G_u} = \frac{1}{P_{G_u}^{\infty}} \int_{\gamma_t}^{\infty} f(\gamma) P_s(\gamma) \, d\gamma \tag{A5a}$$

$$
\begin{aligned}
&= \frac{1}{P_{G_u}^{\infty}} \int_{\gamma_t}^{\infty} \frac{1+K}{\overline{\gamma}} e^{-K} e^{-\frac{(1+K)\gamma}{\overline{\gamma}}} I_0\left(2\sqrt{\frac{K(1+K)\gamma}{\overline{\gamma}}}\right) \\
&\quad \times \sum_{i=0}^{n-2} \binom{n-1}{i+1} (-1)^i \frac{1}{i+2} e^{-\frac{i+1}{i+2}\eta\gamma} \, d\gamma
\end{aligned} \tag{A5b}
$$

$$
\begin{aligned}
&= \frac{1}{P_{G_u}^{\infty}} \sum_{i=0}^{n-2} (-1)^i \binom{n-1}{i+1} \frac{1+K}{(i+2)\overline{\gamma}} e^{-K} \\
&\quad \times \int_{\gamma_t}^{\infty} \exp\left[-\left(\frac{(1+K)}{\overline{\gamma}} + \frac{i+1}{i+2}\eta\right)\gamma\right] I_0\left(2\sqrt{\frac{K(1+K)\gamma}{\overline{\gamma}}}\right) d\gamma
\end{aligned} \tag{A5c}
$$

$$= \frac{1}{P_{G_u}^{\infty}} \sum_{i=0}^{n-2} (-1)^i \binom{n-1}{i+1} \frac{1+K}{(i+2)d_s\overline{\gamma}} \mathrm{e}^{-K}$$
$$\times \int_{\sqrt{2d_s\gamma_t}}^{\infty} x\mathrm{e}^{-\frac{x^2}{2}} I_0\left[\sqrt{\frac{2K(1+K)}{d_s\overline{\gamma}}}x\right] \mathrm{d}x \tag{A5d}$$

$$= \frac{1}{P_{G_u}^{\infty}} \sum_{i=0}^{n-2} (-1)^i \binom{n-1}{i+1} \frac{(1+K)\exp[((1+K)/d_s\overline{\gamma}-1)K]}{(i+2)d_s\overline{\gamma}}$$
$$\times \ Q_1\left(\sqrt{\frac{2K(1+K)}{d_s\overline{\gamma}}}, \sqrt{2d_s\gamma_t}\right) \tag{A5e}$$

Equation (A5d) is obtained by substituting into (A5c) the change of variable, $\gamma = x^2/(2d_s)$, where $d_s = 1/\overline{\gamma} + ((i+1)/(i+2))\eta$. Furthermore,

$$P_{G_u}^{\infty} = \int_{\gamma_t}^{\infty} f(\gamma)\, \mathrm{d}\gamma \tag{A6a}$$

$$= \int_{\gamma_t}^{\infty} \frac{1+K}{\overline{\gamma}} \mathrm{e}^{-K}\mathrm{e}^{-\frac{(1+K)\gamma}{\overline{\gamma}}} I_0\left(2\sqrt{\frac{K(1+K)\gamma}{\overline{\gamma}}}\right) \mathrm{d}\gamma \tag{A6b}$$

$$= \mathrm{e}^{-K} \int_{\sqrt{2(1+K)\gamma_t/\overline{\gamma}}}^{\infty} x\mathrm{e}^{-\frac{x^2}{2}} I_0(\sqrt{2K}x)\, \mathrm{d}x \tag{A6c}$$

$$= Q_1(\sqrt{2K}, \sqrt{2(1+K)\rho}) \tag{A6d}$$

where (A6c) is obtained from (A6b) by the use of the change of variable $\gamma = \overline{\gamma}x^2/2(1+K)$.

REFERENCES

1. Loo C, Butterworth JS. Land mobile satellite channel measurements and modeling. *Proceedings of the IEEE* 1998; **6**:1442–1463.
2. Jahn A. Propagation characteristics for land mobile satellite systems from L-band to EHF-band. *German, ITG-Workshop*, Wessling, May 1998.
3. Karaliopoulos MS, Pavlidou F-N. Modelling the land mobile satellite channel: a review. *Electronics and Communication Engineering Journal* 1999; **11**(5):235–248.
4. Lutz E, Cygan D, Dippold M, Dolainsky F, Papke W. The land mobile satellite communication channel—recording, statistics, and channel model. *IEEE Transactions on Vehicular Technology* 1991; **40**(2):375–386.
5. Sebastiao PJ, Cercas FAB, Cartaxo AVT. Performance of TCH codes in a land mobile satellite channel. *PIMRC 2002*, Lisbon, Portugal. vol. 4, September 2002; 1675–1679.
6. Zhu J, Roy S. Performance of land mobile satellite communication (LMSC) channel with hybrid FEC/ARQ. *Proceedings of GLOBECOM02*, Taipei, Taiwan. 2002; 2851–2854.
7. Ernst H, Donner A, Shabdanov S. Reliable multicast for fixed and land-mobile satellite services. *International Workshop of COST Actions 272 and 280*, ESTEC, Noordwijk. May 2003.
8. Vucetic B, Du J. Channel modeling and simulation in satellite mobile communication systems. *IEEE Journal on Selected Areas in Communications* 1992; **10**(8):1209–1217.
9. Lin HP, Akturan R, Vogel WJ. Satellite-PCS channel simulation in mobile user environments using photogrammetry and Markov chains. *ACM/Baltzer Wireless Networks* 1997; **3**:299–308.

10. Braten LE, Jelta TT. Semi-Markov multistate modeling of the land mobile propagation channel for geostationary satellites. *IEEE Transactions on Antennas and Propagation* 2002; **50**(5):1795–1802.
11. Shen D, Rong J, Yang Y, Quo Y, Cao H, Fu S. The six-state Markov model for land mobile satellite channels. *Proceedings of IEEE MAPE 2005*, Beijing, China. vol. 2, August 2005; 1619–1622.
12. Sakakibara K. Performance analysis of the error-forcasting decoding for interleaved block codes on Gilbert–Elliott channels. *IEEE Transactions on Communications* 2000; **48**(3):386–395.
13. Lee CM. Performance analysis of block codes in hidden Markov channels. *Master Thesis*, Department of Communications Engineering, National Chiao Tung University, Hsinchu, Taiwan, June 2000.
14. Lee CM, Su YT. Errors-and-erasures decoding of block codes in hidden Markov channels. *IEEE Vehicular Technology Conference*, Greece, May 2001.
15. Daraiseh A-GA, Baum CW. Advances on the performance of Reed–Solomon codes. *IEEE Transactions on Communications* 1999; **47**(1):1–5.
16. Sakakibara K, Yamakita J. Performance comparison of imperfect symbol- and bit-interleaving of block codes over GF(2^m) on a Markovian channel. *IEEE Transactions on Communications* 2004; **3**(1):269–277.
17. Lee CM, Su YT., Jeng LD. Performance analysis of block codes in Hidden Markov channels. *IEEE Transactions on Communications*, 2008; **56**(1):1–4.
18. Ahlin L. Coding methods for the mobile radio channel. Presented at the *Nordic Seminar on Digital Land Mobile Communications*, Espoo, Finland, February 1985.
19. Wilhelmsson L, Milstein LB. On the effect of imperfect interleaving for the Gilbert–Elliott channel. *IEEE Transactions on Communications* 1999; **47**(5):681–688.
20. Sharma G, Dholakia A, Hassan AA. Simulation of error trapping decoders on a fading channel. *Proceedings of the 1996 IEEE Vehicular Technology Conference*, Atlanta, GA, 28 April 28–1 May 1996; 1361-1365.
21. Proakis JG. *Digital Communications*. McGraw-Hill: New York, 1989.
22. Viterbi AJ. A robust ratio-threshold technique to mitigate tone and partial band jamming in coded MFSK systems. *1982 IEEE Conference Record of MILCOM*, Boston, MA, 1982; 22.4.1–22.4.5.
23. McCullough RH. The binary regenerative channel. *Bell System Technical Journal* 1968; **47**:1713–1735.
24. Su YT, Jeng L-D. Antijam capability analysis of RS-coded slow frequency-hopped systems. *IEEE Transactions on Communications* 2000; **48**(2):270–281.
25. Li Y, Guan YL. Modified Jakes' model for simulating multiple uncorrelated fading waveforms. *Proceedings of the 2000 IEEE Vehicular Technology Conference*, Tokyo, 15–18 May 2000; 1819–1822.

AUTHORS' BIOGRAPHIES

Chang Ming Lee received the BS and MS in Applied Mathematics and Communications Engineering from the National Chiao Tung University (NCTU), Taipei, Taiwan. He is now a PhD candidate in the Department of Communications Engineering at NCTU. His research interests include coding theory and statistical signal processing.

Yu T. Su received the BSEE degree from Tatung Institute of Technology, Taipei, Taiwan and the PhD degree in electrical engineering from the University of Southern California, Los Angeles, in 1974 and 1983, respectively. From 1983 to 1989, he was a senior system analyst and then a corporate scientist of LinCom Corporation, Los Angeles, where his work involved the design of various measurement and digital satellite communication systems. Since September 1989, he has been with the National Chiao Tung University, Hsinchu, Taiwan, where he was head of the Communications Engineering Department between 2001 and 2003, and was an associate dean of the College of Electrical Engineering and Computer Science from 2004–2008. He is also affiliated with the Microelectronics and Information Systems Research Center of the same university and served as a Deputy Director from 1997 to 2000. His main research interests include communication theory and statistical signal processing.